Supporting Information

Markowitz *et al*. 10.1073/pnas.0803183105

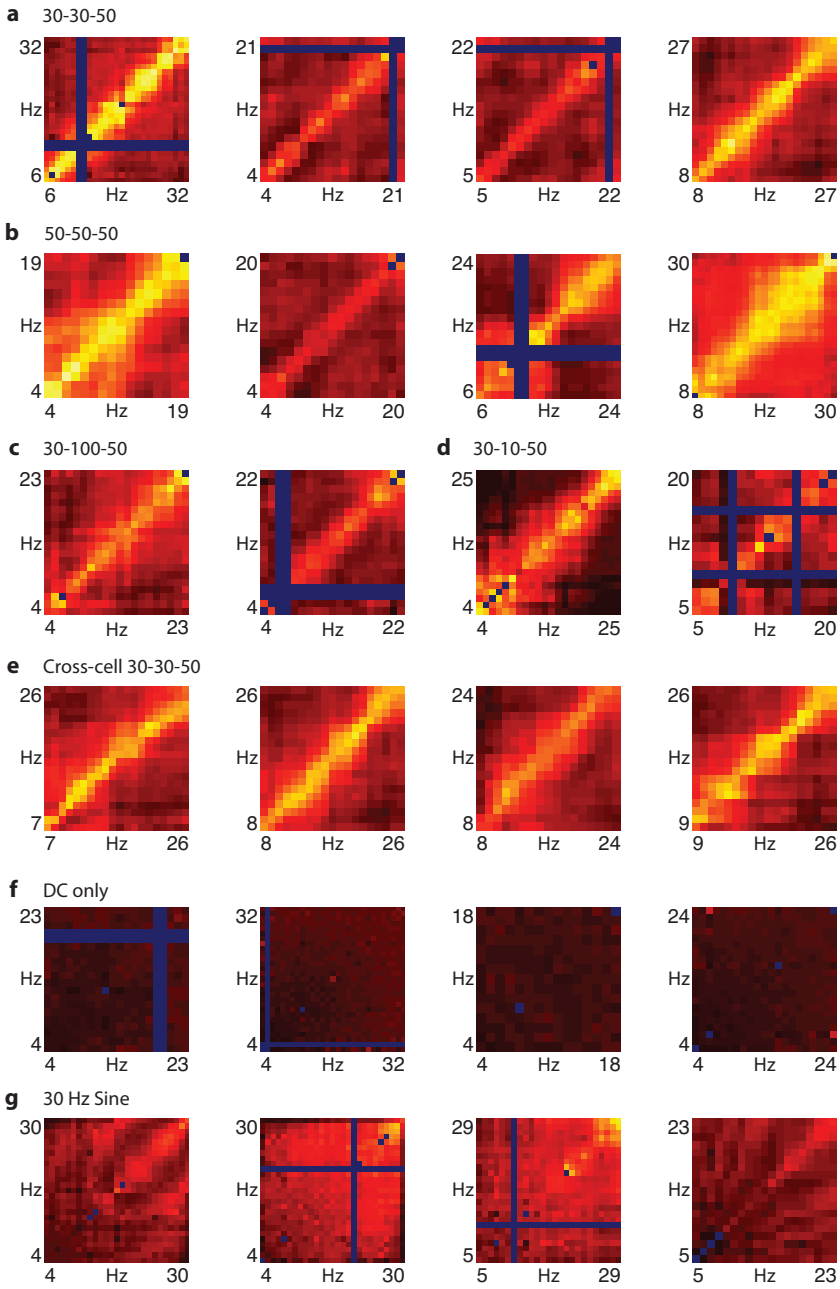

Fig. S1. Other example synchrograms from individual cells with the following parameters. (*a*) F_c = 30 Hz, F_w = 30 Hz, and A_{rms} = 50%; synchrony statistics provided in main text.(*b*) F_c = 50 Hz, F_w = 50 Hz, and A_{rms} = 50%; for n = 7 runs, mean ridge amplitude was 0.55 ± 0.15 and mean ridge/background synchrony was 2.09 ± 0.49. (*c*) F_c = 30 Hz, F_w = 100 Hz, and A_{rms} = 50%. (*d*) F_c = 30 Hz, F_w = 10 Hz, and A_{rms} = 50%. For all stimulus paradigms (range: F_c = 30–50 Hz, F_w = 10–100 Hz; n = 38 runs), mean ridge amplitude was 0.72 ± 0.06 and mean ridge/background synchrony was 2.27 ± 0.84. (e) Other examples of synchrograms from cross-cell comparisons with F_c = 30 Hz, F_w = 30 Hz, and A_{rms} = 50%. (*f* and *g*) Other example synchrograms from control experiments using constant current input only (*f*) and constant current plus 30-Hz sine waves (*g*). Control statistics are provided in the main text. In all panels, unsampled rate–rate combinations are colored blue.

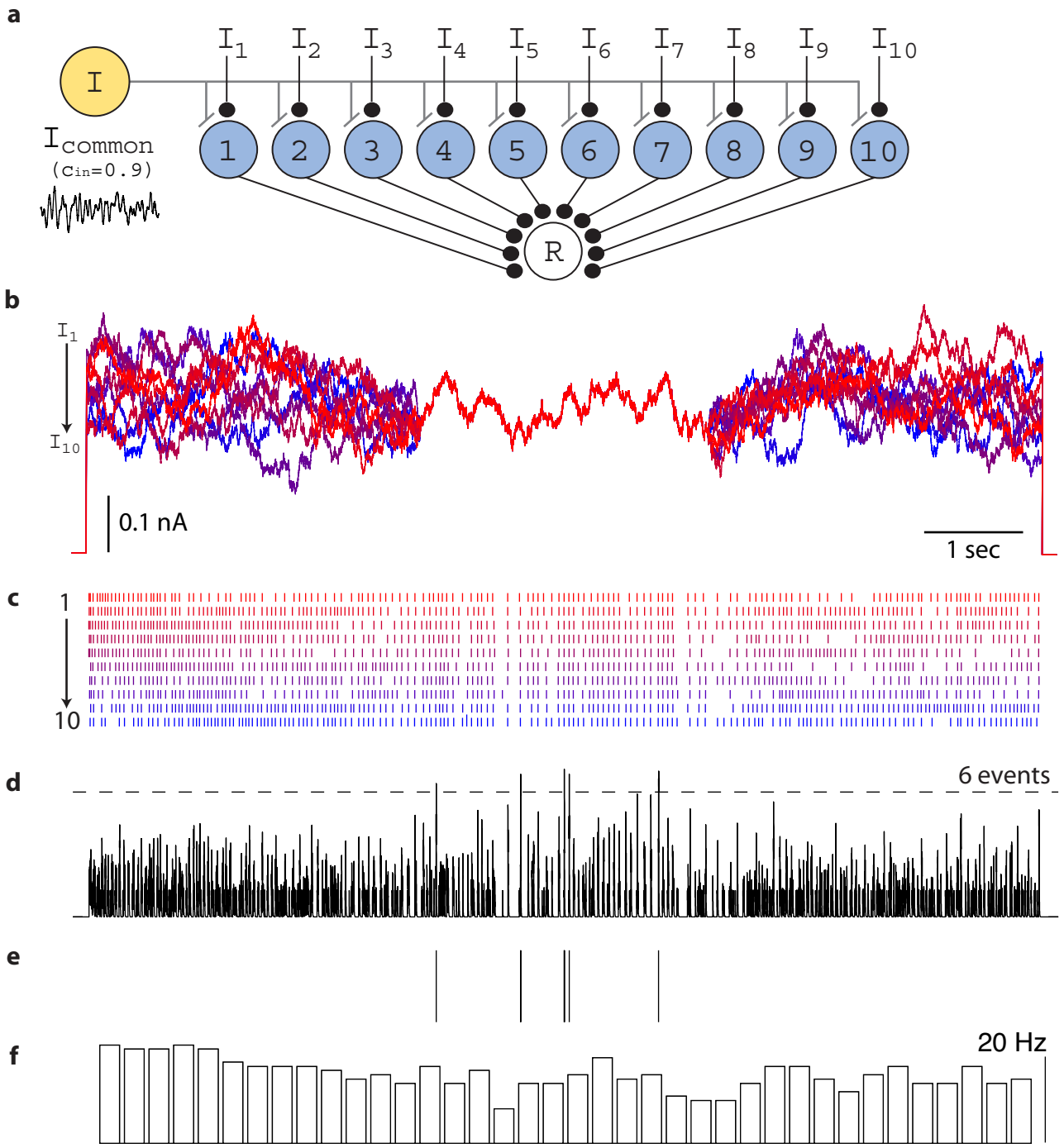

Fig. S2. MAE computation is robust to baseline variability and reduced gamma stimulus correlation. (*a*) Model network used to test MAE computation in the presence of noisy oscillations. Each neuron in the population receives independent time-varying excitatory drive (I_1–I_{10}) and a common oscillatory input (I_{common}). All 10 neurons provide synaptic input to a postsynaptic read-out neuron (R) which reports population synchrony by generating action potentials. (*b*) To reproduce this model experimentally, a single L2/3 cell was injected with 10 waveforms of 10-s duration. During the first 3.5 s, baselines drift independently, each following the dynamics of a Langevin equation with 500-ms time constant; baselines then converge to a common waveform generated by the same process for 3 s, and finally diverge to follow independent trajectories for another 3.5-s interval. Waveforms are color-coded by initial firing rate during the experiment, with high values in red and low values in blue. During the experiment, a frozen noise stimulus with F_c = 30 Hz, F_w = 30 Hz, and A_{rms} = 25% was corrupted by summation with an independently generated gamma waveform during each epoch to yield an ensemble correlation of 0.9 (see *Methods*), and the resulting noise was added to each stimulus waveform from *b*. (*c*) Spike rasters for all 10 stimulus epochs, sorted by increasing initial firing rate and color-coded to match *b*. Stimulus epochs were presented in a random order during the experiment. (*d*) Spike rasters from each stimulus epoch were convolved with the synaptic EPSP kernel and summed to mimic input to a coincidence detector postsynaptic to 10 neurons. A threshold of 6.0 events was applied to detect population synchrony. (*e*) Ticks indicate threshold-crossing events in *d*. Population synchrony is enhanced during the 3-s interval when firing rates are approximately equal, despite a slowly fluctuating baseline and 0.9 correlated gamma stimuli. (*f*) Average firing rate across all 10 epochs, calculated by counting spikes in sequential bins of 220 ms.

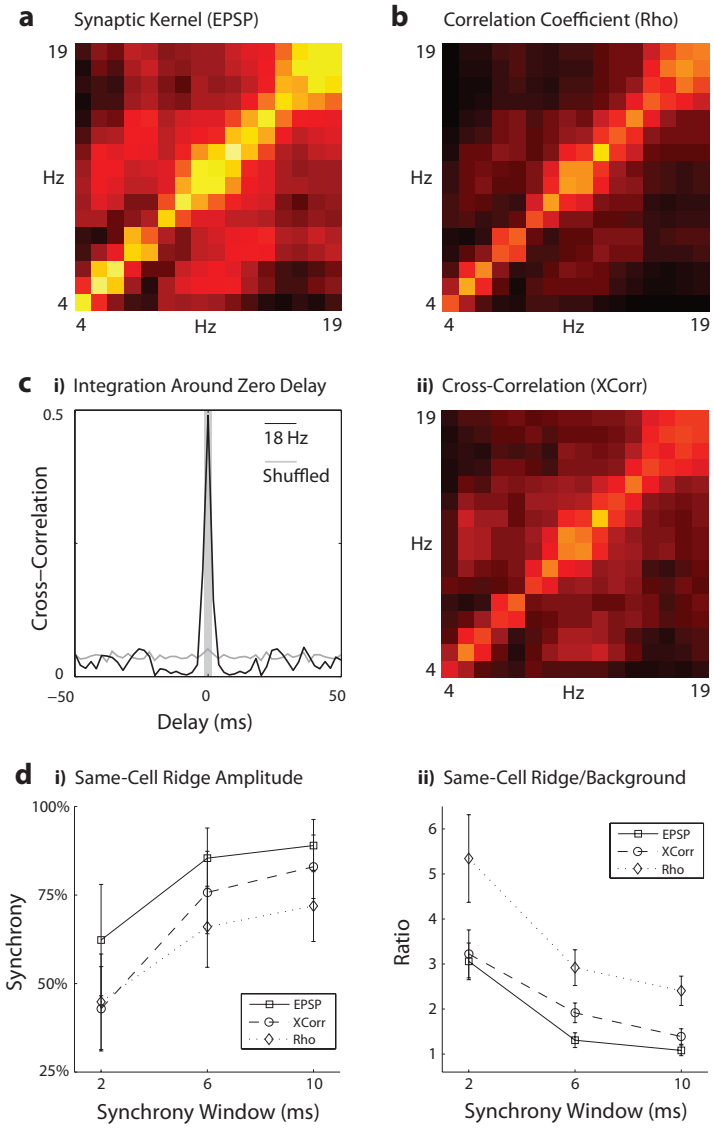

Fig. S3. Rate-specific synchrony is observed using other measures of correlation. All synchrograms generated from experimental data shown in Fig. 1. (*a*) Synchrogram generated by using an EPSP kernel method with a 2-ms synchrony window. (*b*) Synchrogram generated by using methods from the text, with the kernel-based synchrony measure replaced by the correlation coefficient (ρ) measure described in ref. 1. Before each pairwise epoch comparison, spikes were binned by using a sliding window of length $t = 2$ msec to yield spike count vectors n1 and n2. The correlation coefficient was then calculated as:

$$\rho_T = \frac{\langle n_1 n_2 \rangle - \langle n_1 \rangle \langle n_2 \rangle}{\sqrt{\langle n_1^2 \rangle - \langle n_1 \rangle^2} \sqrt{\langle n_2^2 \rangle - \langle n_2 \rangle^2}}.$$

After calculating ρ for each epoch–epoch comparison, measurements were grouped by firing rate and summarized in a synchrogram. (*c*) Cross-correlation also was used to generate synchrograms as an alternative to the methods described previously. A summary cross-correlogram was generated from all spike raster pairs at each rate–rate combination. (i) Example cross-correlogram generated from four rate–rate comparisons at $r_1 = 18$ Hz, $r_2 = 18$ Hz, conditioned on 157 reference spikes. The density of the cross-correlogram was integrated from -2 ms to $+2$ ms (gray bar) to generate a statistic for this rate–rate comparison at 2-ms resolution. (ii) Synchrogram generated using this cross-correlogram based measure of synchrony. (*d*) Summary statistics for $n = 23$ runs using $F_c = 30$ Hz, $F_w = 30$ Hz, and $A_{rms} = 50\%$ stimulus calculated by using the three methods described previously. (i) Ridge amplitude versus synchrony window duration for same-cell comparisons. The kernel-based method consistently estimates higher ridge synchrony than the correlation-coefficient and cross-correlation techniques. (ii) Ridge/background ratio versus synchrony window duration for same-cell comparisons. The kernel-based method consistently estimates lower ratios than the correlation-coefficient and cross-correlation techniques.

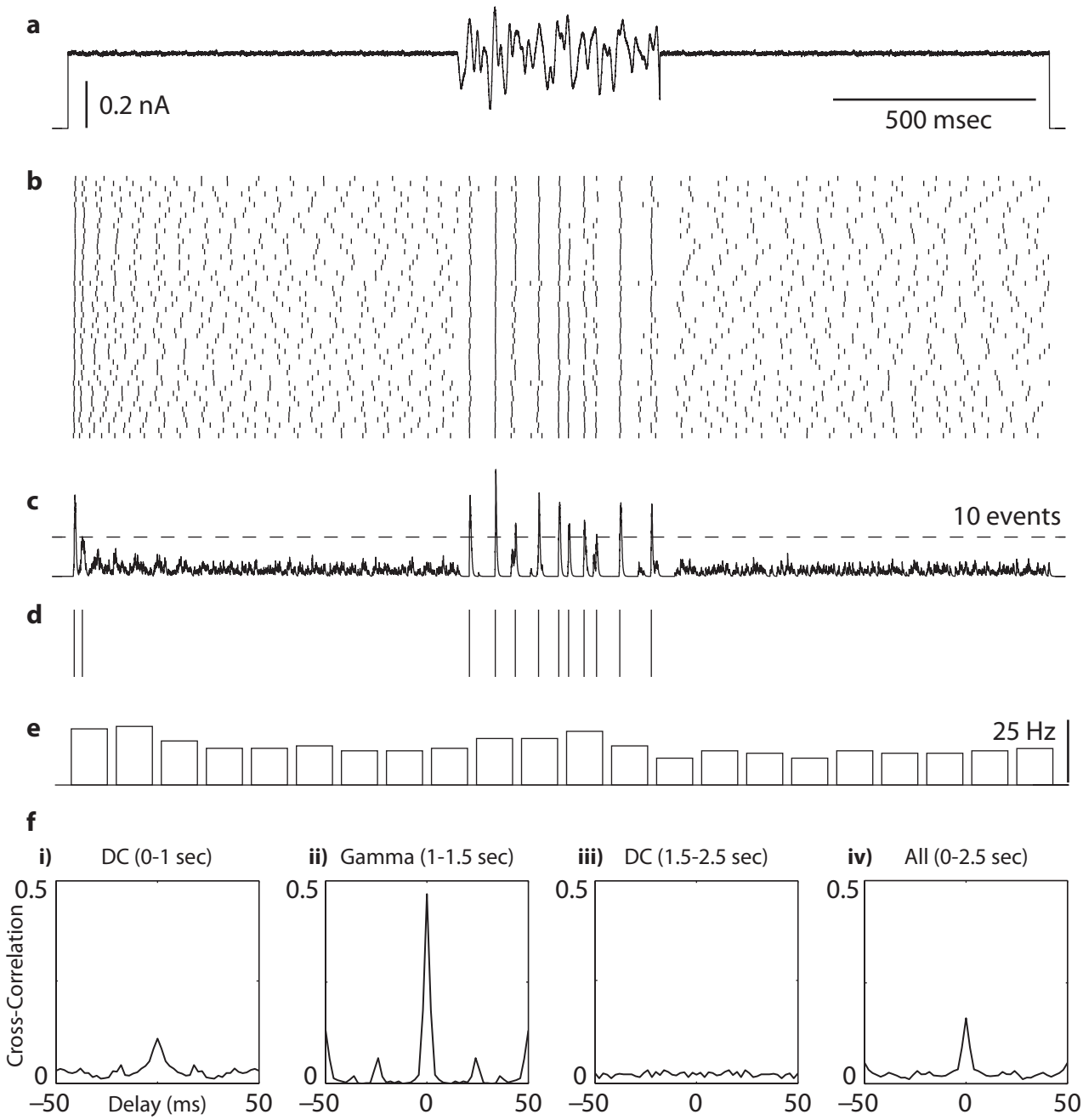

Fig. S4. Synchronous population activity occurs only in the presence of common noisy oscillations. (*a*) A single L2/3 cell was injected with 50 identical waveforms of 2.5-s duration. The repeating waveform consisted of a 0.37-nA step and a 500-ms gamma waveform with F_c = 30 Hz, F_w = 30 Hz, and A_{rms} = 50% added at t = 1 s. (*b*) Spike rasters for all 50 stimulus epochs. (*c*) Spikes from all stimulus epochs were convolved with the synaptic EPSP kernel and summed to mimic input to a coincidence detector postsynaptic to 50 neurons. A threshold of 10 events was applied to detect population synchrony. (*d*) Ticks indicate threshold-crossing events in *c*. Although the same waveform was presented during each epoch, population synchrony emerged only when the noisy gamma stimulus was present. (*e*) Mean population firing rate across all 50 epochs, calculated by counting spikes in sequential 110-ms bins. Noisy gamma does not significantly change population-averaged firing rate, relative to intervals with constant current only. (*f*) Cross-correlograms were generated by pooling relative spike times for all epoch pairs during initial constant step (0–1 s) (i), 500-ms gamma stimulus (1–1.5 s) (ii), late constant step (1.5–2.5 s) (iii), and entire stimulus interval (0–2.5 s) (iv). Peak cross-correlation during the short gamma stimulus (ii) far exceeds maximum values calculated from the constant current only intervals. This peak is significantly attenuated (iv) when data are analyzed by using a longer window containing a mixture of gamma and constant current only stimuli.

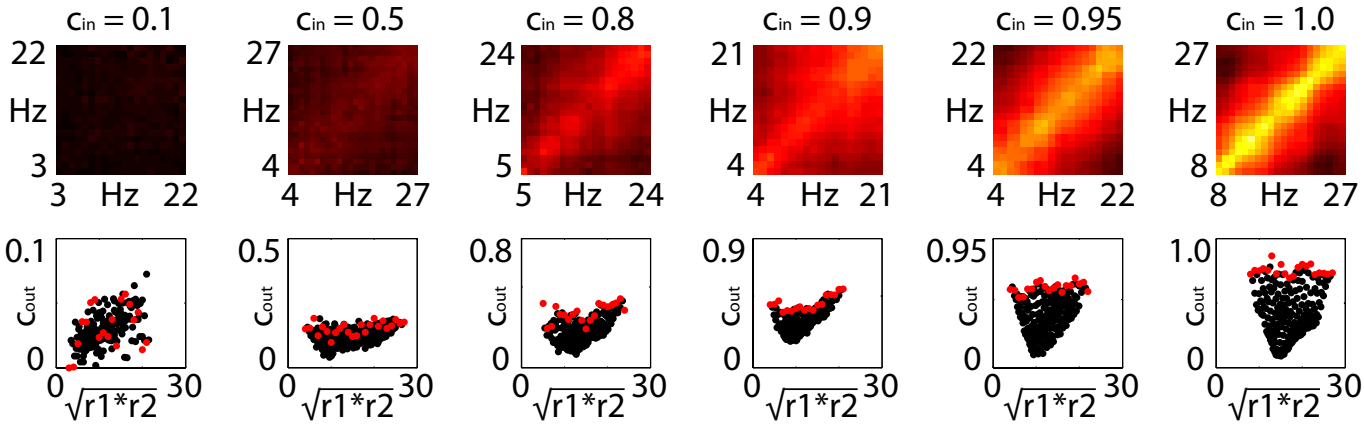

Fig. S5. Output correlation depends on firing rate differences when input stimuli are highly correlated. (*Upper*) All synchrograms were generated by using the correlation-coefficient measure described with t = 10-ms bins. (*Lower*) Each scatterplot shows the output correlation versus the geometric mean of firing rate pairs for all pixels in the corresponding synchrogram. On-diagonal data are plotted in red and off-diagonal data are plotted in black. When stimulus correlation is weak, c_{in} = 0.1, c_{out} increases approximately linearly with the geometric mean of firing rates, as described in ref. 1. As c_{in} increases to 0.8, a ridge begins to appear in the synchrogram and nonlinearity emerges in the c_{out} versus geometric mean scatterplot, suggesting that firing rate difference is now an important determinant of c_{out}. The effect is most pronounced for c_{in} = 1.0. These results demonstrate that rate-specific synchrony emerges with increasing stimulus correlation, and that firing rate difference is more important than geometric mean of firing rates for the determination of c_{out} when c_{in} is high.

1. de la Rocha J, Doiron B, Shea-Brown E, Josic K, Reyes A (2007) Correlation between neural spike trains increaseswith firing rate. *Nature* 448:802–806.